

parameter η , defined²⁴ by

$$\eta = 3[2(2\pi)^3\rho]^{-1} \int d\mathbf{k}' \int d\mathbf{k} \int d\mathbf{P} |(\mathbf{k}' | Qe^{-1}\bar{G}(\mathbf{P}) | \mathbf{k})|^2. \quad (38)$$

The results are given in Fig. 4.

V. CONCLUSIONS

We have seen that equivalent two-body Hamiltonians can give widely different results for the binding energy and equilibrium density of nuclear matter. However, these large changes in energy and density tend to be correlated in an interesting way: An increase in binding energy is accompanied by an increase in equilibrium

density. Our rough calculation in the separation approximation shows why this is true. The saturation curves form a one-parameter family. The parameter characterizes the distortion of the wave function. Thus the softer of two equivalent potentials, which produces less distortion in the wave function, will give a larger binding energy and density. Exact values of the healing parameter η , which is a measure of the distortion in the wave function, have been calculated. These values support the idea that smaller distortion implies larger binding energy and density.

The wide range of results obtainable from equivalent two-body Hamiltonians suggests that nuclear-matter calculations might help to pin down the nature of the nucleon-nucleon potential. Theoretical error bounds on the higher-order corrections to the Brueckner approximation would be essential for that purpose. It is important to emphasize additional theoretical specifications for acceptable potentials and to scrutinize the justification of these specifications.

²⁴ F. Coester and H. Kümmel, Nucl. Phys. **17**, 477 (1960). Brandow's parameter κ (defined in Ref. 3) is related to η by $\kappa = 2\eta$. See also F. Coester, in *Lectures in Theoretical Physics*, edited by K. T. Mahanthappa (Gordon and Breach, Science Publishers, Inc., New York, 1969), Vol. XI.

Nonconservation of Isospin in the $^{14}\text{N}(d, d')^{14}\text{N}$ Reaction*

J. R. DURAY† AND C. P. BROWNE

Department of Physics, University of Notre Dame, Notre Dame, Indiana 46556

(Received 23 October 1969)

The $^{14}\text{N}(d, d')^{14}\text{N}$ reaction to the first excited state of ^{14}N (2.31 MeV, 0^+ , 1) was investigated for isospin nonconservation. Angular distributions were taken for nine incident deuteron energies between 5 and 10 MeV. The symmetries observed in the angular distributions indicate a predominantly compound-nuclear reaction mechanism. The observed violation arises most probably from "Coulomb mixing" in the ^{16}O compound nucleus. The measured cross-section ratio of the first to the second (3.95 MeV, 1^+ , 0) excited state of ^{14}N varied from 3 to 1% for deuteron energy increasing from 6 to 10 MeV. The region of excitation of ^{16}O between 26.0 and 31.0 MeV was investigated by measuring the excitation function for inelastic deuteron scattering to the second excited state of ^{14}N for deuteron energies between 5.9 and 12.2 MeV at a laboratory angle of 60° . Gross structure was observed at excitation energies of 27.2 and 29.6 MeV in ^{16}O . The presented data are compared with photoabsorption data for this range of excitation energy.

I. INTRODUCTION

THIS work was undertaken to study the effects of isospin nonconservation in the $^{14}\text{N}(d, d')^{14}\text{N}$ reaction. Previous deuteron inelastic scattering experiments¹⁻³ involving light nuclei showed no direct evidence of the reaction proceeding to states whose formation is forbidden by isospin conservation. Comparison with the yields to nearby states for which isospin is

conserved typically gave upper limits on the order of a few percent or less.

Preliminary investigations of the $^{14}\text{N}(d, d')^{14}\text{N}$ reaction indicated the feasibility of directly observing the inelastic deuterons that populate the first excited state at 2.31 MeV ($J^\pi = 0^+$, $T = 1$). The primary goal of this study was to find the shape of the angular distribution of the 2.31-MeV level and to measure the cross section as a function of incident deuteron energy. Interest in the energy dependence of the angular distribution of this isospin-nonconserving reaction was stimulated by work done on the $^{12}\text{C}(d, \alpha)^{10}\text{B}$ (1.74 MeV, 0^+ , 1) reaction^{4,5} and more recently on the $^{16}\text{O}(d, \alpha)^{14}\text{N}$ (2.31

* Work supported in part by the U.S. Office of Naval Research under contract No. Nonr 1623(05) and based upon portions of a thesis submitted by J. R. Duray to the Graduate School of the University of Notre Dame in partial fulfillment of the requirements for the Ph.D. degree.

† Present address: The Ohio State University, Columbus, Ohio.

¹ C. K. Bockelman, C. P. Browne, W. W. Buechner, and A. Sperduto, Phys. Rev. **92**, 665 (1953).

² D. W. Miller, B. M. Carmichael, U. C. Gupta, V. K. Rasmussen, and M. B. Sampson, Phys. Rev. **101**, 740 (1956).

³ B. H. Armitage and R. E. Meads, Nucl. Phys. **33**, 494 (1962).

⁴ L. Meyer-Schützmeister, D. von Ehrenstein, and R. G. Allas, Phys. Rev. **147**, 743 (1966).

⁵ J. W. Jänecke, T. Yang, W. S. Gray, and R. Polichar, Phys. Rev. **175**, 1301 (1968).

MeV, $0^+, 1$) reaction.⁶ In both reactions, the isospin-nonconserving groups have forward-peaked angular distributions and resonant structure in their excitation functions for incident deuteron energies corresponding to the main strength of the giant dipole resonance. Below this "threshold," most of the angular distributions are, as expected, symmetrical.

Recently, Noble⁷ tried to explain such behavior of the $T=1$ angular distributions along with a smooth increase in the nonconserving excitation function, and even more recently⁸ he tried to explain such behavior with the resonant energy dependence of the excitation function. The basic problem with which these proposals are concerned is how to relate the excitation function, which exhibits a compound-nuclear behavior, to the forward-peaked angular distribution.

The first excited state of ^{14}N should be a relatively pure $T=1$ state. It is expected⁹ that for very low and very high excitation energies in the compound system, the isospin T will be a good quantum number. The excitation energy in the ^{16}O compound nucleus, corresponding to $^{14}\text{N}+d$, is 20.7 MeV. In this region of broad overlapping states, isospin is expected to be a good quantum number because such states have such short lifetimes that the Coulomb force does not have time to mix components of differing isospin into states initially formed with well-defined isospin. The main strength of the giant dipole lies between the excitation

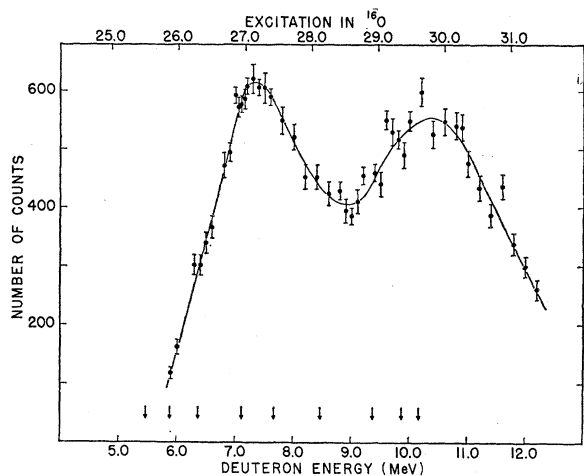


FIG. 1. Excitation function for inelastic deuterons to the second excited state of ^{14}N ($E_x=3.95$ MeV, $J^\pi=1^+$, $T=0$). The laboratory observation angle was 60° . The curve is drawn to aid the eye. Arrows indicate energies at which angular distributions were measured for the first ($T=1$) and second ($T=0$) excited states. The uncertainties indicated are statistical.

⁶ R. M. Polichar, J. Jänecke, T. F. Young, and W. S. Gray, *Bull. Am. Phys. Soc.* **13**, 1425 (1968).

⁷ J. V. Noble, *Phys. Rev.* **162**, 934 (1967); **173**, 1034 (1968).

⁸ J. V. Noble, *Phys. Rev. Letters* **22**, 473 (1969).

⁹ A. M. Lane and R. S. Thomas, *Rev. Mod. Phys.* **30**, 257 (1958).

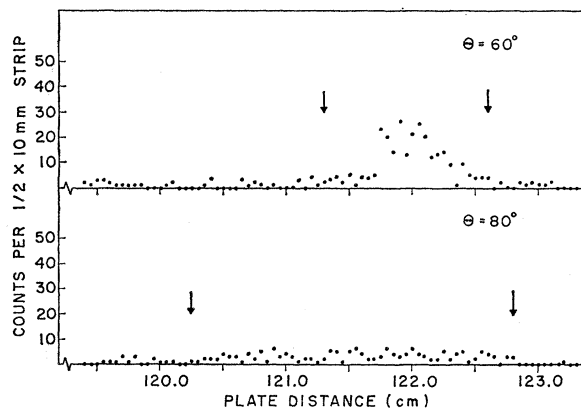


FIG. 2. Examples of the photographic emulsion data of the inelastic deuterons going to the 2.31-MeV state of ^{14}N . The arrows indicate the summation interval used for area extraction as discussed in the text. The bombarding energy was 7.67 MeV. The upper plot shows a run made at 60° and the lower plot a run at 80° .

energies of 22 and 24 MeV in ^{16}O and has relatively pure isospin, as is indicated by a comparison of $^{16}\text{O}(\gamma, p)$ and $^{16}\text{O}(\gamma, n)$ data.^{10,11}

For most cases of nonconservation of isospin, the predominant mechanism for breakdown is considered to be mixing in the compound nucleus. That is to say, a $T=0$ compound state has mixed into it a $T=1$ component (of the same spin and parity) by means of the Coulomb force. For $T=0$ reaction products, then, $T=1$ final states are populated to the degree of the $T=1$ impurity in the compound state. This population will be proportional to the lifetime of the compound state. Although mixing in the compound nucleus is certainly, to some degree, a cause of the nonconservation of isospin, proposals^{4,12,13} not involving mixing in the compound nucleus have been made to explain the unexpectedly large violation that has been observed. These proposals have been concerned mainly with a deuteron-target (or equivalently the deuteron-residual nucleus) electromagnetic interaction.

The $^{14}\text{N}(d, d')^{14}\text{N}$ reaction offers a good test for the proposed deuteron-target interactions. In addition, this reaction proceeds through the giant dipole region of the ^{16}O compound nucleus. Since the observed forward-peaked angular distribution of the $^{12}\text{C}(d, \alpha)^{10}\text{B}$ and $^{16}\text{O}(d, \alpha)^{14}\text{N}$ isospin nonconserving reactions also occur in the giant-dipole-resonance region of ^{14}N and ^{18}F , respectively, the $^{14}\text{N}(d, d')^{14}\text{N}$ reaction can be used to investigate any influence that the giant dipole has on the isospin nonconservation.

¹⁰ N. W. Tanner, G. C. Thomas, and E. D. Earle, *Nucl. Phys.* **52**, 45 (1964).

¹¹ B. C. Cook, J. E. E. Baglin, J. N. Bradford, and J. E. Griffin, *Phys. Rev.* **143**, 712 (1966).

¹² R. J. Drachman, *Phys. Rev. Letters* **17**, 1017 (1966).

¹³ T. A. Griffy, *Phys. Letters* **21**, 694 (1966).

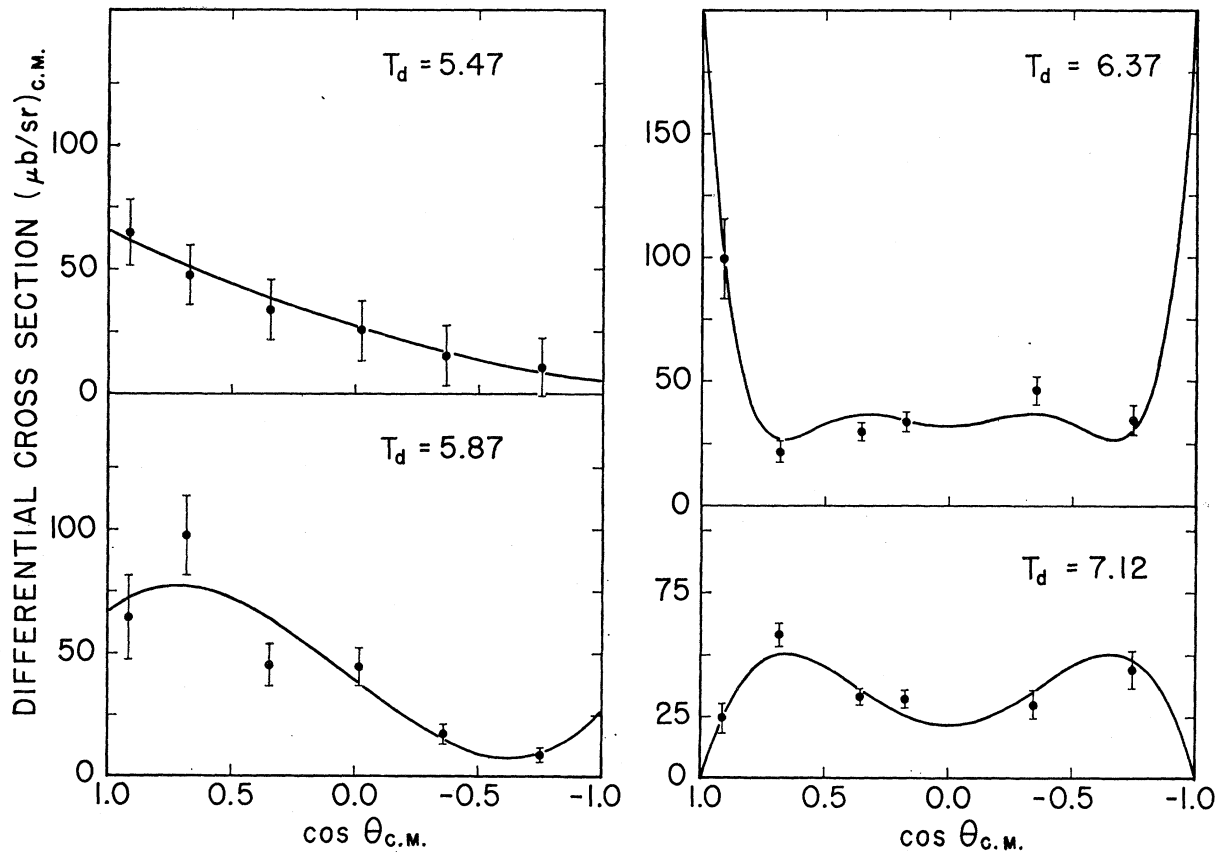


FIG. 3. Angular distributions of inelastic deuterons to the first excited state of ^{14}N ($E_x = 2.31$ MeV, $0^+, 1$). The solid line is the result of a least-squares fit of $\sum a_l P_l(\theta)$. The mean incident deuteron energy T_d , in MeV, is shown on each plot.

II. EXPERIMENTAL PROCEDURE

The facilities of the physics division of the Argonne National Laboratory were used in accumulating the data for this experiment. The nominal energy of the incident deuteron beam from the tandem accelerator was determined by magnetic analysis. The energy resolution of the beam, as defined by the geometry of the entrance and exit slits of the analyzing magnet, was typically 0.15%.

The reaction products were momentum-analyzed by a broad-range magnetic spectrograph of the Browne-Buechner type. Both photographic emulsions and a position-sensitive solid-state detector mounted at the focal surface of the spectrograph were employed as particle detectors.

The ^{14}N target was made by evaporating adenine onto a Formvar and gold backing. Since adenine has a low melting point, target life with few exceptions was short, even though a rotating target holder was used to dissipate the energy loss of the deuteron beam over a large target area. By evaporating the adenine in pill form and using constant evaporator geometry, the targets were found to be reproducible to within $\sim 4\%$ as determined by normalization runs.

The excitation function for the second excited state of ^{14}N was measured with a position-sensitive detector at a laboratory angle of 60° . The deuteron energy was varied from 5.9 to 12.1 MeV in steps of 200 keV. Certain regions of the excitation function were repeated in 100-keV steps. The 2.31- and 3.95-MeV groups were recorded simultaneously on photographic emulsions for incident deuteron energies (T_d) of 6.37, 7.12, 7.67, 8.46, 9.37, 9.87, and 10.16 MeV. The momentum range of the spectrograph was not sufficient to allow simultaneous recording of both groups at lower deuteron bombarding energies. Consequently, only the angular distributions of the 2.31-MeV state were measured for deuteron energies of 5.47 and 5.87 MeV. Typically, runs were made at laboratory angles of 20° , 40° , 60° , 80° , and 130° .

The identification of the deuterons was readily made from the track length in the emulsion and the measured momentum. To enhance the yield of the 2.31-MeV group, a fairly thick nitrogen target was used. Energy loss in the target broadened the observed groups and slightly decreased their energy. From the position of the strong 3.95-MeV group on the photographic emulsion, the input deuteron energy was determined and then used to find the expected position of the weak

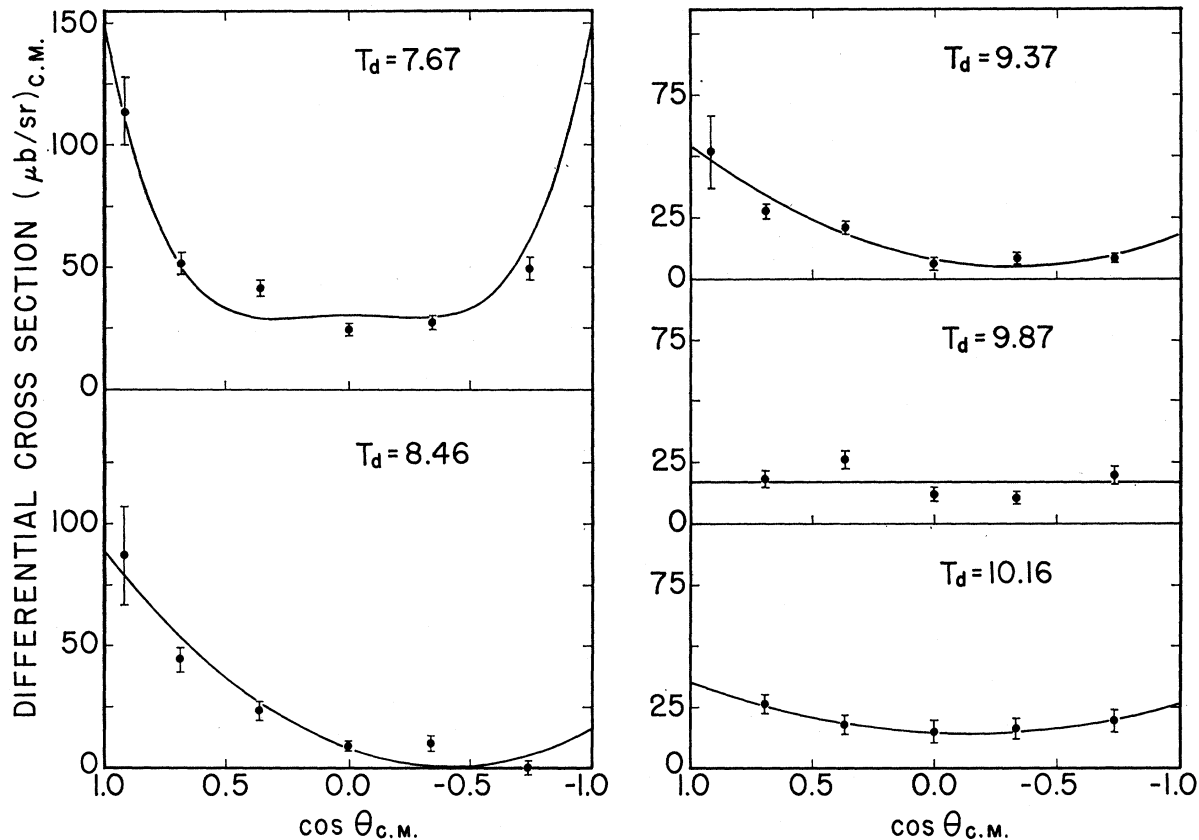


FIG. 4. Angular distributions of inelastic deuterons to the first excited state of ^{14}N ($E_x=2.31$ MeV, 0^+ , 1). The solid line is the result of a least-squares fit of $\sum a_l P_l(\theta)$. The mean incident deuteron energy T_d , in MeV, is shown on each plot.

2.31-MeV group. Since this group arose from an isospin-forbidden reaction, it was very weak and hence often difficult to observe above background. The width of the 3.95-MeV group was used in conjunction with a relative stopping-power curve to estimate the proper summation interval for the 2.31-MeV group. For a given angular distribution, the normalization of one angle to another was made through the ground-state protons from the $^{14}\text{N}(d, p)^{15}\text{N}$ reaction that struck a fixed solid-state detector. The angular distributions at different energies were normalized to one another by means of the excitation function of the 3.95-MeV state. The angular distributions were then converted to differential cross section using the measurement of Green and Middleton.¹⁴ Their value was 1 mb/sr at 60° in the laboratory for a 9.0-MeV deuteron energy. The uncertainty in this number, taken from their data, was about 25%. This uncertainty has not been included in the errors quoted herein.

III. RESULTS

Figure 1 shows the excitation function obtained for the second excited state (3.95 MeV). Arrows are

¹⁴T. S. Green and R. Middleton, Proc. Phys. Soc. (London) A69, 28 (1956).

placed on the figure to show energies at which angular distributions were measured for the first (2.31 MeV) and second excited states. Typical data for the forbidden 2.31-MeV group are shown in Fig. 2. The proper summation interval obtained from the strong 3.95-MeV group, as explained above, is shown by arrows in Fig. 2. The back-angle data, of which the lower portion of Fig. 2 is indicative, would not have lent itself to an unambiguous area extraction had not this procedure been employed. The large difference in summation interval between 60° and 80° seen in Fig. 2 comes from the use of different targets for the two angles. The input energies calculated from the positions of the 3.95-MeV group varied by no more than 0.2% for a complete angular distribution. This variation arose primarily from changes in target position from reflection to transmission. The proper summation interval for the 2.31-MeV group was always known quite accurately.

The angular distributions were fitted by least squares to a sum of Legendre polynomials of the form

$$d\sigma/d\Omega = \sum_l a_l P_l(\theta).$$

The results of these fits for the 2.31-MeV state are indicated by the solid lines in Figs. 3 and 4. The

TABLE I. Coefficients for the least-squares fit of Legendre polynomials to the angular distributions of the 2.31-MeV level of ^{14}N . The indicated uncertainty is the standard error. The units are $\mu\text{b}/4\pi\text{ sr}$.

Deuteron energy (MeV)	a_0	a_1	a_2	a_3	a_4	a_5	a_6
5.47	29.9 ± 2.0	30.8 ± 4.1	5.4 ± 5.3				
5.87	41.9 ± 13.0	42.5 ± 23.4	5.3 ± 33.6	-23.0 ± 41.2			
6.37	46.3 ± 5.7		51.3 ± 15.8		64.2 ± 20.2		36.7 ± 36.2
7.12	35.5 ± 3.7		0.7 ± 8.4		-35.4 ± 13.0		
7.67	51.1 ± 4.3		65.9 ± 9.9		32.9 ± 14.4		
8.46	22.8 ± 5.1	36.7 ± 9.3	29.7 ± 12.1				
9.37	17.4 ± 2.6	17.9 ± 4.8	18.7 ± 6.2				
9.87	17.4 ± 3.3						
10.16	20.0 ± 1.0	4.6 ± 1.8	10.7 ± 2.8				

criterion for acceptability for these fits was a minimum in the standard deviation of the fit as a function of the number of fit parameters. In Fig. 5, the solid lines show the fits for the 3.95-MeV state. No acceptable fit could be made to the 3.95-MeV angular distributions for deuteron energies of 8.46 and 9.37 MeV. The dashed curves through these data in Fig. 5 serve merely as a guide. The incident deuteron energy indicated is the mean of the energies from the individual runs. The deviation from the mean was less than 0.2%. The coefficients determined by the least-squares fits are tabulated in Table I for the first excited state of ^{14}N and in Table II for the second excited state. Figures 6 and 7 are plots of the total cross section of inelastic deuterons to the isospin-“forbidden” 2.31-MeV state and the “allowed” 3.95-MeV state of ^{14}N , respectively. The total cross sections at $T_d=8.46$ and 9.37 were estimated by means of a planimeter since no acceptable least-squares fit could be made.

IV. DISCUSSION

A. Isospin Nonconservation

In practice, the “degree” of nonconservation of isospin, or the amount of $T=1$ impurity present, is obtained by comparing the forbidden cross section with

an allowed cross section at a comparable final-state excitation energy. There are, however, four factors which should be considered in determining the forbidden-to-allowed ratio.

The first of these factors is the influence of the final-state spins and parities. Many of the forbidden transitions that have been investigated are of the 0^+ to 0^+ type, which occur frequently in (d, α) reactions. Hashimoto and Alford¹⁵ first pointed this out, noting that the statistical factors alone would result in a lower cross section than for, say, a 0^+ to a 3^+ transition.

The second factor to be considered is the penetrability. This effect is normally small when the energies of the reaction products are well above the barrier and the allowed and forbidden groups correspond to comparable excitation energies. If the reaction under consideration proceeds through a region of high density of compound-nuclear states, the statistical relation for the cross section given by Hauser and Feshbach¹⁶ can be used to correct the observed ratio. The calculation includes not only the usually small effects of penetrability but the statistical effect of the spin and parity of the final state.

The remaining two factors are not so easily taken into account but are nevertheless significant in some cases. The most important but highly elusive effect of

TABLE II. Coefficients for the least-squares fit of Legendre polynomials to the angular distributions of the 3.95-MeV level of ^{14}N . The indicated uncertainty is the standard error. Units are $\text{mb}/4\pi\text{ sr}$.

Deuteron energy (MeV)	a_0	a_1	a_2	a_3	a_4
6.37	0.68 ± 0.04	0.19 ± 0.08			
7.12	1.56 ± 0.06	-0.39 ± 0.10	0.32 ± 0.15	-0.21 ± 0.19	
7.67	1.45 ± 0.03		0.17 ± 0.07		0.49 ± 0.10
8.46	no fit				
9.37	no fit				
9.87	1.32 ± 0.08		0.78 ± 0.18		0.46 ± 0.26
10.16	1.62 ± 0.11		0.97 ± 0.25		0.96 ± 0.37

¹⁵ V. Hashimoto and W. Parker Alford, Phys. Rev. **116**, 981 (1959).

¹⁶ W. Hauser and H. Feshbach, Phys. Rev. **87**, 366 (1952).

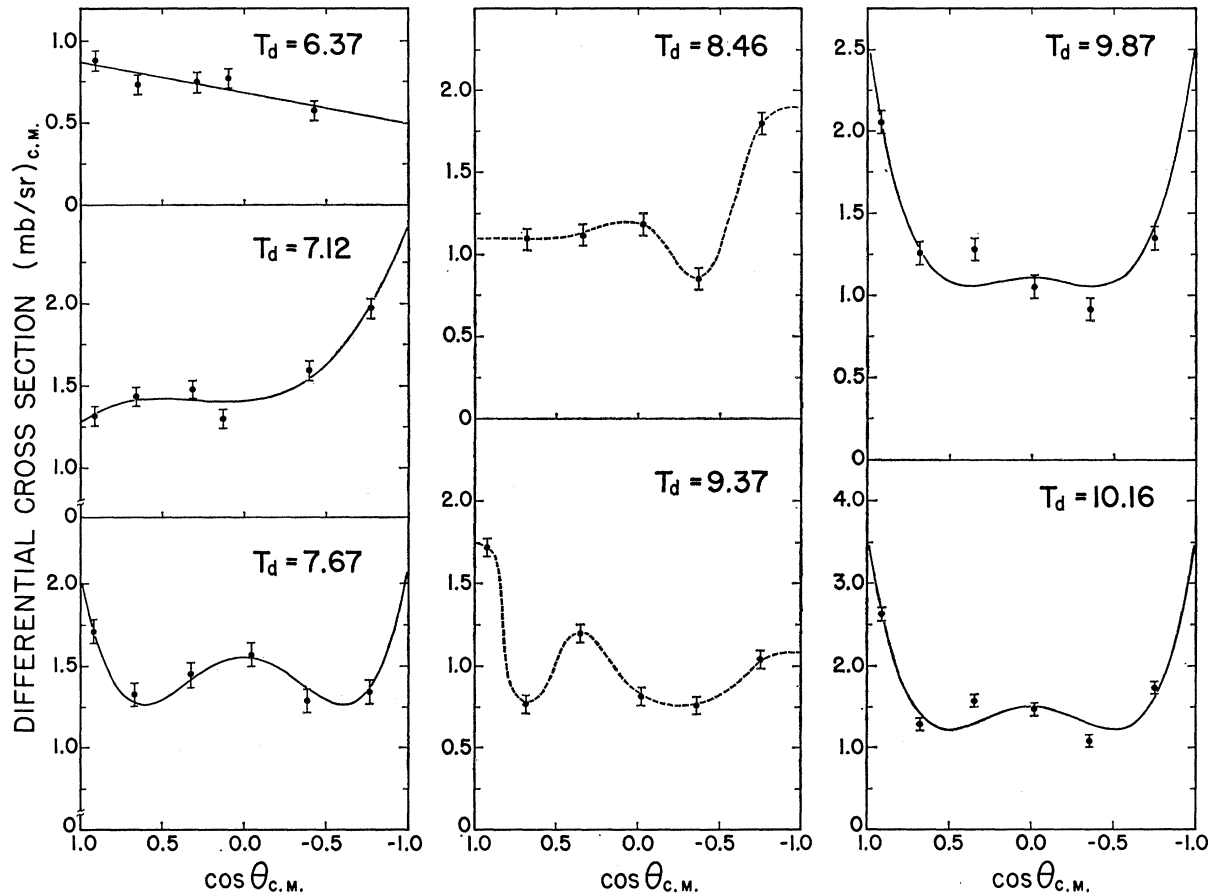


FIG. 5. Angular distributions of inelastic deuterons to the second excited state of ^{14}N ($E_x=3.95$ MeV, 1^+ , 0). The solid line is a least-squares fit of $\sum_j a_j P_j(\theta)$. The incident deuteron energy T_d , in MeV, is shown on each plot. The dashed curves for $T_d=8.46$ and 9.37 MeV indicate that no fit could be made.

the two is the amount of direct reaction contributing to the intensity of the allowed group used in measuring the ratio. Certainly such an effect should be taken into account, but at this time there is no reliable method for doing so.

The fourth and last factor that should be considered

TABLE III. Measured isospin impurities for incident deuteron energies between 6 and 10 MeV. The ratio R is $\sigma(2.31)/\sigma(3.95)$, i.e., the ratio of the $T=1$ to $T=0$ cross section.

Deuteron energy (MeV)	R (%)
6.37	6.7 ± 1.2^a
7.12	2.3 ± 0.3
7.67	3.5 ± 0.4
8.46	1.8 ± 0.4
9.37	1.7 ± 0.3
9.87	1.3 ± 0.3
10.16	1.2 ± 0.1

^a See text for penetrability estimate.

is that of the different configurations of the final states. Accurate estimates are difficult to obtain since they require detailed spectroscopic information. A crude estimate of the effect may be obtained from isospin-allowed scattering data.

The inelastic scattering of deuterons has an advantage that most isospin-nonconserving (d, α) reactions do not have, viz., no spin inhibition is involved. The correction usually made when restrictions from angular momentum effects are present has, however, the advantage of correcting for penetrability effects as well. In the present work, penetrability corrections were applied only to the data at $T_d=6.37$ MeV.

For inelastic deuterons going to the 3.95-MeV state, the Coulomb barrier in the exit channel corresponds to an input deuteron energy of 7.0 MeV. In order to estimate the penetrability for the $T_d=6.37$ MeV case, the square-well (5.14 fm) transmission coefficients were calculated using Coulomb functions tabulated by Gove.¹⁷ The ratio of the coefficients for the 3.95-MeV

¹⁷ W. T. Sharp, H. E. Gove, and E. B. Paul, *Graphs of Coulomb Functions* (Atomic Energy of Canada Limited, Chalk River, Canada, 1955).

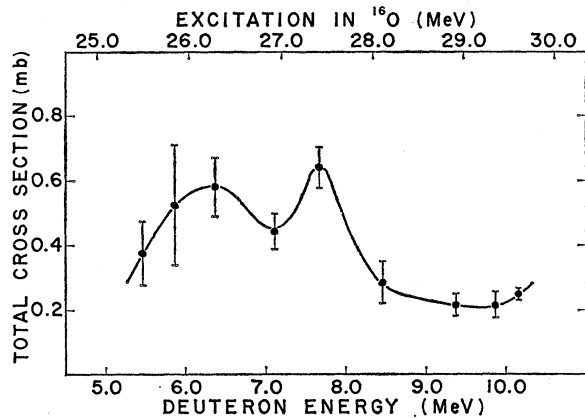


FIG. 6. Total cross section of inelastic deuterons to the first excited (2.31 MeV) state of ^{14}N . The curve is drawn as a guide.

level indicates a reduction of about 50% in the 3.95-MeV cross section. This then reduces the measured ratio at $T_d=6.37$ MeV by a factor of 2. For incident deuteron energies greater than 7.0 MeV, the exit-channel penetrability correction was small. The observed cross-section ratios, i.e., the ratio $\sigma(2.31)/\sigma(3.95)$, are shown in Table III.

The measured ratios are all of the order of a few percent. This would seemingly indicate the approximate validity of isospin as a good quantum number for this reaction proceeding through this region of excitation in the ^{16}O compound nucleus. The angular distributions to the 3.95-MeV level at $T_d=9.37$, 9.87, and 10.16 MeV may indicate some forward peaking, but, in the absence of data at very large angles, this is uncertain. The lack of fits at $T_d=8.46$ and 9.37 MeV and the very different shapes make an interpretation of forward peaking even less tenable. In any case, contributions from direct reaction do not appear to be appreciable.

The effect of different configurations for the first and second excited states of ^{14}N could have a pronounced effect on the measured ratio. The configuration for the 2.31-MeV (0^+ , 1) state is generally¹⁸⁻²⁰ thought to be $p_{1/2}^2$. The 3.95-MeV (1^+ , 0) state is considered to be core excited, viz., having a $p_{3/2}^{-1}p_{1/2}^{-1}$ configuration with a possible $p_{1/2}^2$ admixture. Ideally, it would be desirable to know what the cross-section ratio would be in the absence of isospin conservation. For an extremely crude estimate of the effect of final-state configurations in the present (d, d') work, we look to (p, p') scattering data from ^{14}N . A comparison cannot be taken too seriously since different intermediate nuclei are involved.

Bockelman *et al.*,¹ for $\theta_{\text{lab}}=90^\circ$ and a proton energy of 7.5 MeV, measured $d\sigma(2.31)/d\sigma(3.95)$ to be about

¹⁸ W. W. True, Phys. Rev. **130**, 1530 (1963).

¹⁹ E. K. Warburton and W. T. Pinkston, Phys. Rev. **118**, 733 (1960).

²⁰ I. Talmi and I. Unna, Phys. Rev. **112**, 452 (1958).

0.5. Earwaker and Hebbard²¹ measured this ratio as 0.1 at three laboratory angles for proton energies from 9.3 to 10.5 MeV. At 10.5 MeV, Oda²² measures the same ratio as <0.1 . For larger proton energies, the data indicate a sizable direct-reaction contribution although the ratio remains roughly 0.1 or less. These rather large differences in $\sigma(2.31)/\sigma(3.95)$ for the (p, p') case do not necessarily indicate that such differences in yield would occur for the (d, d') case with no isospin restriction. The difference in final-state population observed in the (p, p') data is brought out to suggest the possibility that a similar effect could exist in the (d, d') case. If this and the previously discussed effects are present to an appreciable extent in the present (d, d') case, the measured yield ratio underestimates the isospin impurity.

Using the recipe of Barker and Mann²³ and comparing $^{16}\text{O}(\gamma, n)$ and $^{16}\text{O}(\gamma, p)$ data,¹¹ an isospin impurity (i.e., the $T=0$ amplitude) of $\approx 0.25\%$ for excitation energies between 27.5 and 29.0 MeV in ^{16}O is estimated. This amplitude was used to approximate the $T=1$ amplitude in predominantly $T=0$ states of the same excitation energy. Applying MacDonald's ground-state estimate²⁴ to the 2.31-MeV state of ^{14}N and using 0.25% for ^{16}O , an impurity of 1% or less in the $^{14}\text{N}(d, d')$ reaction is calculated. These estimates from the photoabsorption data and MacDonald's ground-state esti-

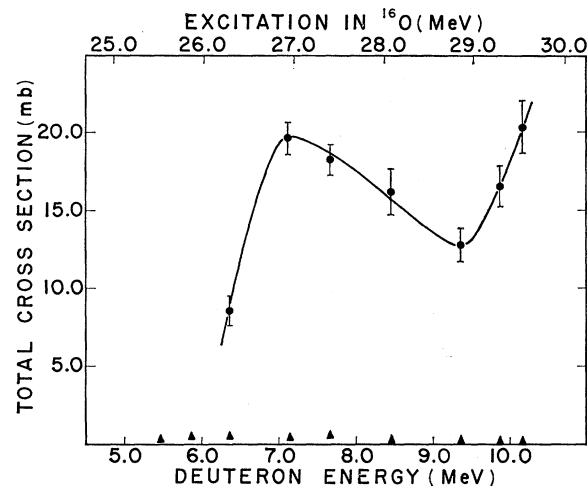


FIG. 7. The total cross section of inelastic deuteron scattering to the second excited state of ^{14}N is shown by the solid circles. The cross section of the first excited state is indicated by the triangles on the same scale for comparison. The curve is drawn as a guide.

²¹ L. G. Earwaker and D. F. Hebbard, Nucl. Phys. **53**, 252 (1964).

²² Y. Oda, M. Takenda, N. Tokano, T. Yamazaki, C. Hu, K. Kikuchi, S. Kobayashi, K. Matsuda, and Y. Nagahara, J. Phys. Soc. Japan **15**, 760 (1960).

²³ F. C. Barker and A. K. Mann, Phil. Mag. **2**, 5 (1957).

²⁴ W. M. MacDonald, in *Nuclear Spectroscopy*, edited by F. Ajzenberg-Selove (Academic Press Inc., New York, 1960), Part B, pp. 932.

mate, however, do not reflect the variation with energy of the impurity that is measured. Estimates^{12,13} have been made of the $T=1$ amplitude in the deuteron wavefunction. These estimates are based on a virtual excitation of the deuteron from the deuteron-target electromagnetic interaction. (The original estimate in Ref. 13 for the $T=1$ amplitude of the deuteron contains a numerical error. The correct amplitude should be $2.5 Z \times 10^{-3}$.) But here again there is no energy dependence of the $T=1$ impurity.

The isospin impurities measured in this experiment should be considered as lower limits in view of the possible contribution of the four effects previously outlined. The observance of structure in the excitation function taken at 60° (Fig. 8) and in the total cross section (Fig. 6) along with the symmetries observed in the angular distributions are indicative of a compound-nucleus reaction mechanism. If the above effects are significant, the mixing in the compound nucleus is much greater than the 0.25% estimated from the photoabsorption data. Only mixing in the compound nucleus could account, however, for the variation with energy.

The "direct reaction" phenomenon reported in the $^{12}\text{C}(d, \alpha)^{10}\text{B}$ reaction^{4,5} and the $^{16}\text{O}(d, \alpha)^{14}\text{N}$ reaction⁶ is not obviously present in the $^{14}\text{N}(d, d')^{14}\text{N}$ reaction. Broad structure is seen centered at about $T_d=6.2$ MeV in the 2.31-MeV, $T=1$ cross section, which corresponds to ~ 26 -MeV excitation in ^{16}O . This region is slightly higher than the main strength of the giant dipole resonance, although structure is obviously apparent in photoabsorption data¹¹ with an intensity of about 40% of the main peak at 22.3 MeV. There is a possible indication of resonant structure at $T_d=7.6$ MeV that corresponds to about 27 MeV in ^{16}O . More data would be required, however, to substantiate this. Noble's recent proposal concerning forward peaking in the nonconserved cross section⁸ does not apply in the (d, d') case since we observe no forward peaking in the 2.31-MeV cross section. However, the region of excitation in the compound nucleus is comparable, viz., the energy region of the giant dipole.

For the incident energies where the nonconserved forward-peaked angular distributions in the $^{12}\text{C}(d, \alpha)^{10}\text{B}$ reaction are observed, the isospin-conserved angular distributions of the ground, first, and third excited states are also forward peaked.⁴ The reaction mechanism for the $^{14}\text{N}(d, d')^{14}\text{N}$ reaction is that of the compound nucleus for both the first ($T=1$) and the second ($T=0$) excited states of ^{14}N . In both the (d, d') and the (d, α) reactions, structure is observed in the nonconserved cross sections corresponding to the giant dipole region of excitation. On this basis, we suggest that a mechanism for "mixing" of isospin in the compound nucleus could be an interaction with the bulk properties of the giant dipole, i.e., with its deformed and/or oscillatory²⁵ character.

²⁵ M. Goldhaber and E. Teller, Phys. Rev. **74**, 1046 (1948).

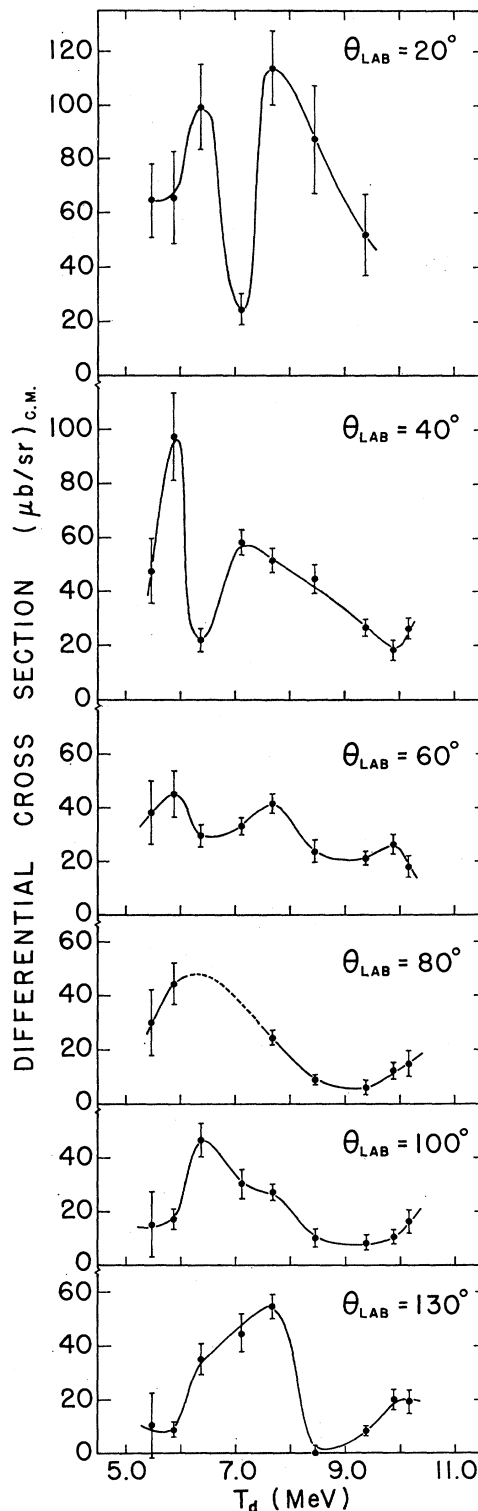


FIG. 8. Data from the angular distributions of Figs. 3 and 4 plotted as excitation functions for various angles. The curves are drawn as an aid.

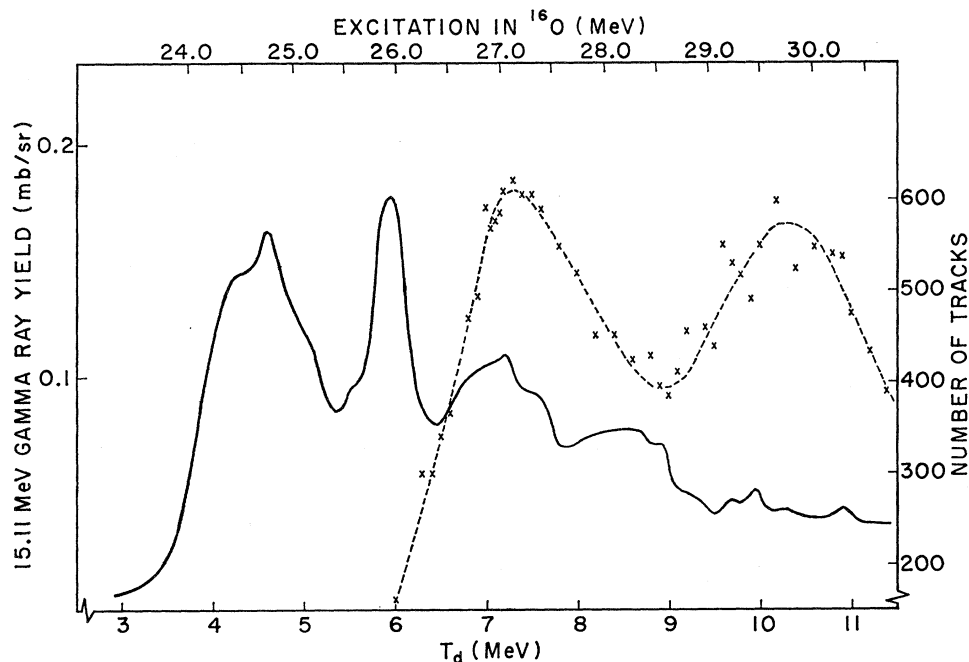


FIG. 9. Comparison of the $^{14}\text{N}(d, \alpha)^{12}\text{C}(15.11 \text{ MeV}, 1^+, 1)$ yield curve to the $^{14}\text{N}(d, d')^{14}\text{N}(3.95 \text{ MeV}, 1^+, 0)$ yield curve taken at 60° in the lab. The solid line indicates the (d, α) data and is plotted against the left-hand ordinate scale, whereas the (d, d') data indicated by crosses are plotted against the right-hand ordinate scale (note suppressed zero). Roughly 400 counts correspond to 1 mb/sr.

In Fig. 8, we show the variation with energy of the differential cross section for the 2.31-MeV data for constant angles. The variations in the ratio $d\sigma(2.31)/d\sigma(3.95)$ for a fixed angle are more apparent than the variation of the total cross-section ratio with energy. The four factors discussed earlier are also more sensitive when the ratio is taken for a fixed angle. In general, the ratios for the forward angles are higher than those given in Table III by about a factor of 2. The back angles are down relative to the Table III values by about the same amount.

It is of interest to compare the violation observed in the (d, d') reaction with that observed in the $^{14}\text{N}(d, \alpha)^{12}\text{C}(E_x=15.1 \text{ MeV}, 1^+, 1)$ reaction.²⁶ In both reactions, the same region of excitation in ^{16}O was covered, and neither is restricted by angular-momentum considerations. It would be expected that the violation observed in both reactions would be about the same if the nonconservation arose from "mixing" in the compound nucleus. In the (d, α) reaction, the state in ^{12}C used in measuring the ratio was the 12.71-MeV ($1^+, 0$) state. The measured impurity of 3% for $T_d=7.1 \text{ MeV}$ was attributed to "mixing" in the compound nucleus. In the (d, d') reaction, the ratio for the same incident deuteron energy was measured as 2.3%. This agreement with the (d, α) data suggests, then, that differences in the configuration of the first and second

excited states of ^{14}N play a relatively minor part in the measured ratio. It would be necessary to measure the cross section for the 2.31-MeV state in finer energy steps to compare it properly with the resonance structure seen in the $^{14}\text{N}(d, \alpha)^{12}\text{C}(15.1 \text{ MeV})$ reaction. The angular distributions measured in the present work and the agreement with the (d, α) reaction as to the amount of violation seem to indicate a compound-nucleus reaction. Further work on the two reactions is planned with a view to comparison of excitation functions.

B. States in ^{16}O

The excitation energies covered in ^{16}O by the 60° yield curve of the 3.95-MeV state ranged from 26 to 31 MeV. Although these data are taken for one laboratory angle, the general trend of the total cross section for this level suggests that the gross behavior of the 60° excitation function is similar to that of the total cross section.

A tabulation of existing data on the structure of ^{16}O in the excitation energy range 26–30 MeV is presented in Table IV. The isospin-conserved $^{14}\text{N}(d, \alpha)^{12}\text{C}$ data are given in the first three columns as they were presented by Chaudhri.²⁷ Correspondence with other data that are tabulated is indicated when there is agree-

²⁶ C. P. Browne, W. A. Schier, and I. F. Wright, Nucl. Phys. 66, 49 (1965).

²⁷ M. A. Chaudhri and L. Lassen, in *Congres International de Physique Nucleaire* (Editions du Centre National de la Recherche Scientifique, Paris, 1964), Vol. II, 321I/C253.

TABLE IV. Structure observed in ^{16}O for the excitation energy range 26–30 MeV. The symbols α_0 , α_1 , and α_2 refer to α particles going to the ground state and first and second excited states of ^{12}C , respectively. The symbols d_1 and d_2 refer to inelastic deuterons measured in this experiment going to the first and second excited states of ^{14}N . “A(l)” indicates an asymmetry in the angular distribution that was least-squares fitted with all orders of Legendre polynomials up to order l . “S(l)” indicates symmetry in the angular distribution for even orders only of Legendre polynomials up to order l .

$^{14}\text{N}(d, \alpha)^{12}\text{C}$ reaction ^a			$^{14}\text{N}(d, \alpha)^{12}\text{C}$ reaction ^b	$^{16}\text{O}(\gamma, n)^{15}\text{O}$ reaction ^c	$^{16}\text{O}(\gamma, n)^{16}\text{O}$ reaction ^d	$^{13}\text{C}(^3\text{He}, \alpha_0)^{12}\text{C}$ reaction ^e	$^{14}\text{N}(d, d')^{14}\text{N}$ d_1 d_2	
α_0	α_1	α_2						
26.1	26.0	26.0	25.94					
					26.2			
				26.38			S(6)	A(1)
26.5	26.6	26.5						
(27.0) ^f	26.95	27.1	27.0				S(4)	A(3)
27.4	27.3	27.4	27.4 ^g	27.45	27.3		S(4)	S(4)
27.75	27.65					27.6		
27.9	27.9	28.0						
			28.2					
28.35								
			28.5 ^g	28.55				
28.65	28.7	28.6						
28.95	28.95				28.9		A(2)	
29.3		29.4	29.4 ^g				S(0)	S(4)
29.6	29.75	29.85		29.6			A(2)	S(4)
	30.3	30.1	30.2 ^g					

^a See text, Ref. 27.

^b α -particle group leading to 15.11-MeV state in ^{12}C . See text, Ref. 26.

^c See text, Ref. 11.

^d See text, Ref. 28.

^e See text, Ref. 29.

^f Structure indicated by data but not stated in text of paper.

^g Considered doubtful; see Ref. 27.

ment by an arbitrarily chosen value of ± 100 keV. The structure in the $^{14}\text{N}(d, \alpha)^{12}\text{C}^*$ reaction²⁶ is that observed in the nonconserved component. Results of two measurements^{11,28} of the $^{16}\text{O}(\gamma, n)^{15}\text{O}$ reaction are listed in columns 5 and 6. The most recent observation of structure in ^{16}O was with the $^{13}\text{C}(^3\text{He}, \alpha_0)^{12}\text{C}$ reaction.²⁹ The structure observed at 27.6 MeV in ^{16}O was identified as a $J^\pi = 3^-, T = 0$ state. The last two columns in Table IV indicate, to within 100 keV, the correspondence of the angular distributions of the (d, d') reaction with excitation energy in ^{16}O . This correspondence does not necessarily indicate that structure was observed in the present work, but rather shows where angular distributions were measured and what the results were of the least-squares analysis. Angular distributions corresponding to excitation energies of 25.6, 26.0, and 28.1 MeV are not included in Table IV. An “A” indicates that both even and odd orders of Legendre polynomials were used to fit the distribution, the highest order being indicated in parenthesis. An “S” indicates that only even orders were used, with the maximum order l given in parenthesis. A similar table has been presented by Suffert³⁰ for excitation energies of 20–25 MeV in ^{16}O .

²⁸ J. T. Caldwell, R. R. Harvey, R. L. Bramblett, and S. C. Fultz, Phys. Letters **6**, 213 (1963).

²⁹ H. R. Weller, N. R. Roberson, and D. R. Tilley, Phys. Letters **25B**, 541 (1967).

³⁰ M. Suffert, Nucl. Phys. **75**, 226 (1966).

In Fig. 9, the 60° excitation function of inelastic deuterons to the 3.95-MeV state is compared with the excitation function obtained from the $^{14}\text{N}(d, \alpha)^{12}\text{C}^*$ (15.1 MeV, $1^+, 1$) reaction.²⁶ In the latter, the total cross section was measured by the 15.11-MeV $M1$ radiation going to the ground state.

An interesting feature of Table IV is the correspondence between the isospin-conserved and the nonconserved (d, α) reaction of Refs. 27 and 26, respectively. In the conserved reaction, corresponding structure was seen at all angles at which data were taken. The nonconserved reaction, on the other hand, does not contain all the structure seen in the conserved (d, α) reaction. Nevertheless, surprising correspondence is seen, which suggests that the nonconserved reaction is selective in its resonance. One possibility for the selectivity is that the observed resonances arise from appreciable concentration of $T=1$ impurities in a relatively high density of wide $T=0$ compound states of the same spin and parity.

The main strength of the giant dipole resonance in ^{16}O is concentrated in two prominent peaks in the (γ, n) and (γ, p) data that correspond to excitation energies of 22.2 and 24.1 MeV. In the vicinity of 24.1 MeV in ^{16}O ($T_d \approx 3.9$ MeV), the conserved (d, α) cross section of Ref. 27 exhibits very sharp dips. Although the nonconserved (d, α) data of Ref. 26 are influenced somewhat by the Coulomb barrier at this deuteron energy, the yield is also down (but beginning to in-

crease), peaking at the first resonance observed in the excitation function at $T_d=4.3-4.6$ MeV (see Fig. 9). Suffert has observed resonant structure in the $^{14}\text{N}(d, \gamma)^{16}\text{O}$ reaction corresponding to 22.7 MeV in ^{16}O . This structure lies in the valley of the two most prominent photoabsorption resonances. The (d, γ_0) reaction should be isospin conserving. The fact that a prominent resonance is observed is attributed³⁰ to the reaction proceeding through an isospin impurity in the compound nucleus.

The nonconserving (d, α) cross section in Fig. 9 exhibits pronounced structure for deuteron energies from 4.3 to about 9.0 MeV, above which the cross section is down by more than a factor of 2 from that at 7.0 MeV. The tapering off of the structure could arise from the fact that the excitation energy in ^{16}O is being further removed from the main strength of the giant dipole resonance. In the (d, α) data of Fig. 9, this tapering off is nicely fitted by

$$\sigma = (7.2 \times 10^3) / (E_x - 22.0)^2$$

for $E_x \geq 26.0$ MeV. This could imply that all or part of the structure observed is due to an interaction involving the giant dipole. Gillet and Bloch,³¹ trying to account for the "fine structure" that appears throughout the giant dipole region, have suggested that there exist a number of low-lying 2-particle-2-hole (2p-2h) states that, through configuration mixing (i.e., through an interaction with the 1p-1h state describing the giant dipole) can yield structure. The results³² of calculations predict 2p-2h quasibound states at 23.0, 23.9, 24.4, and 26.0 MeV in ^{16}O . These four quasibound states are formed by the mixing of configurations with the following spins and parities: $0^+(0) - 1^-(1)$, $2^+(0) - 3^-(1)$, $2^+(0) - 2^-(1)$, and $2^+(0) - 1^-(1)$, respectively, where isospin is indicated in parenthesis. The structure observed in Fig. 9 at 24.7 and 25.9 MeV could correspond to these states.

Off the giant dipole resonance, the structure in the photoabsorption yield becomes weaker, and contributions from $M1$ and $E2$ absorption are probably present along with the dominant $E1$ absorption. There may be a correspondence (in Table IV) of the (d, d') data with that of photoabsorption. It must be emphasized that correspondence of the excitation function and the angular distributions with structure in the giant dipole could be coincidental, in which case the following would be of no consequence.

The gross structure in the 60° excitation function for the 3.95-MeV state is peaked at $T_d=7.4$ and 10.1 MeV, which corresponds to 27.2 and 29.6 MeV, respectively, in ^{16}O . Because of the large input energy increments ($\Delta T_d=100-200$ keV), the observed structure could come from a contribution of a number of resonances in ^{16}O . In particular, for $T_d=7.67$ MeV ($E_x=27.4$ MeV), both the 2.31- and 3.95-MeV angular distributions were fitted with even orders of $P_l(\theta)$ (up to and including $l=4$). The weak assumption that orbital angular momentum in the exit channel does not limit the distribution implies that the spin of the compound state must be >2 . The correspondence with photoabsorption structure would imply that the spin of this resonance at 27.4 MeV in ^{16}O is 2^+ , according to the assumption that along with $E1$, only $M1$ and $E2$ absorption make significant contributions. Discounting this correspondence with the photoabsorption structure, the symmetry in the angular distributions could be due to the reported²⁹ $J^\pi=3^-$ resonance at $E_x=27.6$ MeV ($\Gamma \approx 0.6$ MeV). However, the $^{14}\text{N}(d, \alpha_0)^{12}\text{C}$ reaction²⁷ clearly shows two well-resolved groups at $E_x=27.4$ and 27.75 MeV.

Near 29.6 MeV in ^{16}O ($T_d \approx 10.16$ MeV), the angular distributions (for $T_d=9.8$ and 10.1 MeV) were nearly symmetrical. The 3.95-MeV distributions show a slight asymmetry in the scatter of the 60° and 100° data points, which is assumed to be due to some direct-reaction contribution. At $T_d=10.1$ MeV, the 2.31-MeV angular distribution is indicated in Table IV as being asymmetric. The highest l value involved in the fit is 2. The fit to the 3.95-MeV distribution at $T_d=10.1$ MeV puts a lower limit of 2 on the spin, which is compatible with the 2.31-MeV distribution that indicates the spin to be >1 . By the same correspondence as before, this suggests a 2^+ assignment for $E_x=29.6$ MeV in ^{16}O .

The total cross section of the 2.31-MeV level in Fig. 6 shows an indication of structure at $E_x=27.4$ MeV, whereas the 3.95-MeV cross section in Fig. 7 (similar to the 60° excitation function of Fig. 1) shows broad structure almost 2 MeV wide. The structure observed at $T_d=6.0$ MeV ($E_x=25.9$ MeV) is probably analogous to that observed in the $^{14}\text{N}(d, \alpha)^{12}\text{C}$ reaction shown in Fig. 9.

ACKNOWLEDGMENTS

We wish to express our appreciation to the staff of the physics division of the Argonne National Laboratory for the use of their tandem accelerator under the cooperative program. We also wish to acknowledge the assistance of Dr. J. J. Kroepfl, Dr. F. H. O'Donnell, Dr. A. A. Rollefson, Dr. W. D. Callender, and G. L. Marolt. We are grateful for the careful plate scanning of Patricia G. Huston and Ilde M. Molnar.

³¹ V. Gillet and C. Bloch, Phys. Letters **18**, 58 (1965).

³² V. Gillet, M. A. Melkanoff, and J. Raynal, Nucl. Phys. **A97**, 631 (1967).